

Article

A C-Type Lectin, RfCTL27, Activates the Immune Defense in the Red Palm Weevil *Rhynchophorus ferrugineus* (A.G. Olivier, 1791) (Coleoptera: Curculionidae: Dryophthorinae) by the Recognition of Gram-Negative Bacteria

Yanru Gong^{1,2}, Yongjian Xia^{1,2}, Zhiping Su^{1,2}, Xinghong Wang^{1,2}, Yishuo Kou^{1,2}, Bing Ma^{1,2}, Youming Hou^{1,2} 
and Zhanghong Shi^{1,2,*} 

- ¹ State Key Laboratory of Ecological Pest Control for Fujian and Taiwan Crops, College of Plant Protection, Fuzhou 350002, China; gyr17852843301@163.com (Y.G.); xyj990819@163.com (Y.X.); m17820288537@163.com (Z.S.); 18285120070@163.com (X.W.); kys0511@163.com (Y.K.); ma15534605636@163.com (B.M.); ymhou@fafu.edu.cn (Y.H.)
- ² Ministerial and Provincial Joint Innovation Centre for Safety Production of Cross-Strait Crops, Fujian Agriculture and Forestry University, Fuzhou 350002, China
- * Correspondence: shizh@fafu.edu.cn

Simple Summary: Red palm weevil (RPW), *Rhynchophorus ferrugineus* (Olivier), is an invasive and highly destructive insect pest that poses a significant threat to palm trees. Currently, employing the biological agents are the important alternative method to fight against the infestation and alleviate the pesticide resistance of this pest. However, the control effect is unsatisfactory. It has been well known that the innate immunity plays the vital role for the protection of insect pests upon the attack of pathogens. In this research, we aimed to investigate the role of a C-type lectin, RfCTL27, in the immune response of RPWs. RT-qPCR showed that *Escherichia coli* induced a significant increase in the expression of RfCTL27 in the gut and fat body. After RfCTL27 was silenced, the expression level of antimicrobial peptide (AMP) genes in the gut and fat body was significantly decreased. Therefore, our findings indicate that RfCTL27 is involved in both systemic and gut local immunity by controlling the expression of AMP genes upon the exposure of Gram-negative bacteria.



Citation: Gong, Y.; Xia, Y.; Su, Z.; Wang, X.; Kou, Y.; Ma, B.; Hou, Y.; Shi, Z. A C-Type Lectin, RfCTL27, Activates the Immune Defense in the Red Palm Weevil *Rhynchophorus ferrugineus* (A.G. Olivier, 1791) (Coleoptera: Curculionidae: Dryophthorinae) by the Recognition of Gram-Negative Bacteria. *Insects* **2024**, *15*, 212. <https://doi.org/10.3390/insects15030212>

Academic Editor: Travis Glare

Received: 7 February 2024

Revised: 17 March 2024

Accepted: 19 March 2024

Published: 21 March 2024



Copyright: © 2024 by the authors. Licensee MDPI, Basel, Switzerland. This article is an open access article distributed under the terms and conditions of the Creative Commons Attribution (CC BY) license (<https://creativecommons.org/licenses/by/4.0/>).

Abstract: Red palm weevil, *Rhynchophorus ferrugineus* (Olivier), is a palm tree insect pest that causes significant damage in the many countries from the Indian sub-continent and southeast Asia into date palm-growing countries of Africa, the Middle East, and the Mediterranean Basin. This study is aimed at determining the role of a C-type lectin, RfCTL27, in the immune defense of RPW larvae. RfCTL27 is a secreted protein that possesses a QPD motif, being integral for the discrimination of Gram-negative bacteria. The abundance of RfCTL27 transcripts in the gut and fat body was significantly higher than that in other tissues. Six hours after injection of *Escherichia coli*, the expression level of RfCTL27 in the gut of RPW larvae was significantly elevated compared with other groups. At 12 h after injection of *E. coli*, the expression of RfCTL27 in fat body was dramatically induced in contrast with other treatments. More interestingly, the ability of RPW larvae to clear the pathogenic bacteria in the body cavity and gut was markedly impaired by the silencing of RfCTL27. Additionally, the expression levels of two antimicrobial peptide genes, RfCecropin in the gut and RfDefensin in fat body of RPW larvae, were significantly decreased. Taken together, these data suggested that RfCTL27 can recognize the Gram-negative bacterium and activate the expression of antimicrobial peptides to remove the invaded bacterial pathogens. This study provides a new scientific basis for improving the control efficiency of pathogenic microorganisms against red palm weevils in production practice.

Keywords: invasive pest; pattern recognition receptor; insect immunity; antimicrobial peptide

1. Introduction

Red palm weevil (RPW), *Rhynchophorus ferrugineus* Olivier (Coleoptera: Curculionidae), is an alien destructive insect pest that seriously attacks palm trees and crops, such as sugarcane, and it has caused huge economic loss [1]. Currently, the primary strategy for controlling this pest is through the use of chemical pesticides. Unfortunately, increasing evidence has shown that *R. ferrugineus* has strong resistance to a variety of commonly used pesticides [2,3]. In the perspective of sustainable development, it is emergent to invent a novel alternative management strategy to fight against this pest. To date, certain biological agents, such as the entomopathogenic fungus *Beauveria bassiana* (Bals.-Criv.) Vuill. and bacterium *Serratia marcescens* J have been intensively found to have insecticidal activity against RPW larvae by bioassays in laboratory [4,5]. However, the control efficiency of these biological agents on *R. ferrugineus* in field is still out of our expectation [6]. It is well known that the innate immunity plays the vital role for the protection of insect pests upon the attack of pathogens. In this context, the elucidation of mechanisms by how insect pests activate their innate immunity to fight against the invaded pathogens is of great importance to improve the control efficiency of biological agents. The issuing of RPW genomic data [7] and the intensive usage of RNA-seq [5,8] advanced the identification of immunity-related genes of *R. ferrugineus*. Although some pattern recognition receptors (PRRs) have been determined by RNA silencing [9], the mechanisms underlying how the immune system of *R. ferrugineus* works upon the challenge of pathogens are still far from well known.

C-type lectins (CTLs) belong to a superfamily of proteins that are characterized by the presence of one or more C-type lectin-like domains (CTLDs, also known as carbohydrate-recognition domains, CRDs). These domains have the unique ability to recognize a variety of ligands and play a pivotal role in regulating animal immunity and maintaining homeostasis [10]. The CRD can specifically bind to galactose in the bacterial cell wall to recognize pathogens and activate immune responses in *Tribolium castaneum* [11]. Similar results have been reported in *Drosophila melanogaster* [12] and *Manduca sexta* [13]. These molecules can bind to carbohydrates in a Ca²⁺-dependent manner through conserved motifs, including EPN (Glu-Pro-Asn) and QPD (Gln-Pro-Asp), within the CTLD [13,14]. According to their structure, CTLs are usually classified into three families: the CTL-S family (single CRD), immulectin with dual-CRDs (the IML family), and the CTL-X family (many CRDs with other functional domains) [10]. It has been well verified that CTLs can function as PRRs to mediate animal immune responses, such as opsonization, nodule formation, encapsulation, melanization, and the production of antimicrobial peptides [10,15]. In this study, we combined RT-qPCR, RNAi, and the bioassays on the clearing ability of the invading pathogenic bacterium to validate the function of a CTL gene, *RfCTL27*, in the immune response of *R. ferrugineus*.

2. Materials and Methods

2.1. Red Palm Weevil Rearing and Breeding

Red palm weevil adults were bred in the incubator, and the parameters were set to a temperature of 27 ± 1 °C, photoperiod of 12L: 12D, and relative humidity of 75 ± 5%. Red palm weevil adults were bred in plastic boxes (7 cm in diameter, 10 cm high) and fed with fresh sugarcane chips, which were changed every 3 to 4 days. Female adults laid eggs in sugarcane chips. Then, the sugarcane chips were carefully dissected, and the eggs were collected with a brush and transferred to the Petri dish. Freshly hatched larvae were fed with fresh sugarcane chips. For this pest, the infestation of palm trees was mainly from the larval stage. Therefore, the healthy 4th instar larvae of RPW were selected for uncovering their immunity to the exposure of pathogenic microbes.

2.2. Sequence Characterization of *RfCTL27*

A C-type lectin (*RfCTL27*) was identified in the genome of the red palm weevil and validated by gene cloning. The Open Reading Frames (ORFs) finding tool (<https://www.ncbi.nlm.nih.gov/orffinder/>, accessed on 19 May 2023) and ExPASy-Translate tool (<https://>

web.expasy.org/translate/, accessed on 19 May 2023) were used to predict the open reading frame and the encoded amino acid sequence of RfCTL27. To determine the presence of functional motifs and conservative active sites, we conducted multiple sequence alignments of RfCTL27 using MEGA-X and ClustalX 2.0. Then, we employed PhyloSuite 1.22 and IQtree software to construct phylogenetic trees of RfCTL27 and other insect homologous proteins using the maximum likelihood method. Finally, FiguresTree 1.4.4 software was used to beautify the trees.

2.3. Analysis of RfCTL27 Expression in Different Tissues of the RPW Larvae

The 4th instar larvae of the RPW were dissected to obtain the head, cuticle, fat body, foregut, mid- and hindgut, and hemolymph. Three biological replicates were taken from each tissue, each containing three RPW 4th instar larvae. Then, total RNA was extracted from the above different tissues using Eastep[®] Super Total RNA Extraction-LS1041. The concentration of total RNA was detected by NanoDrop 2000. RT-qPCR reverse transcription kit X0402 was used to prepare the template of cDNA. The reaction system was as follows: 4 μ L 5 \times FasKing-RT SuperMix, 1 μ g total RNA, and added RNase-free water to 20 μ L. Primers for RT-qPCR were designed using Primer 3.0.

RT-qPCR was performed with Taq Pro Universal SYBR qPCR Master MixQ712-02. The RT-qPCRs were conducted with the following protocol: denaturation at 96 $^{\circ}$ C for 10 min, followed by 40 cycles of denaturation at 96 $^{\circ}$ C for 15 s, and annealing at 59 $^{\circ}$ C for 1 min. The RT-qPCR reaction system is shown in Table 1. *Rf β -Actin* was used as an internal control in the experiment. The RT-qPCR data were calculated by $2^{-\Delta\Delta C_t}$ method.

Table 1. The composition of RT-qPCR reaction system.

Reagent	Dosage
SYBR mix	10 μ L
Forward primer	0.4 μ L
Reverse primer	0.4 μ L
cDNA	1 μ L
ddH ₂ O	8.2 μ L
Total	20 μ L

2.4. Expression of RfCTL27 in the Gut and Fat Body of RPW Larvae Challenge with Pathogenic Microbes

To determine whether RfCTL27 was involved in the immune response of RPW larvae against pathogenic microbe infection, the Gram-negative bacterium *Escherichia coli* E and Gram-positive bacterium *Staphylococcus aureus* Rosenbach were used to challenge RPW larvae by abdominal injection. *E. coli* and *S. aureus* were cultured overnight at 37 $^{\circ}$ C with OD₆₀₀ = 0.65 in Luria–Bertani (LB) medium (10 g/L tryptone, 5 g/L yeast extract, 10 g/L NaCl, and pH 7.2). To prepare the bacterial suspension for challenging RPW larvae, 1 mL of bacterial solution was centrifuged at 5000 \times g for 8 min at 4 $^{\circ}$ C, and the supernatant was discarded. Then, the cell pellet was washed with 1 mL of sterilized PBS three times. Finally, the cell pellet was resuspended in PBS to make bacterial suspension with OD₆₀₀ = 1.60. To challenge the RPW 4th instar larvae, 1 μ L of bacterial suspension was injected into the body cavity. Totals of 6, 12, and 24 h after infection, the gut and fat body of these treated larvae were collected for total RNA extraction. Three biological replicates were set in each treatment, and each replicate contained four RPW larvae. RT-qPCR was employed to determine the expression level of RfCTL27, as described in Section 2.3.

2.5. The Impact of RfCTL27 Knockdown on RPW Larvae Immune Response and the Count of Gut eGFP-Labeled *E. coli* Colonies

Double-strand RNA (dsRNA) primers (Table 2) were designed using the E-RNAi (<https://www.dkfz.de/signaling/e-rnai3/>, accessed on 3 August 2023). RfCTL27 and eGFP dsRNA were synthesized using MEGAscript[®] Kit. eGFP dsRNA was used as a

control. For gene silencing, 1 μL of dsRNA (1000 ng/ μL) was injected into the fourth–fifth intersegmental membrane of the RPW 4th instar larvae. Three biological replicates were set, each containing four insects. Then 48 h of dsRNA injection, the gut and fat body were dissected.

Table 2. The primers were used for RT-qPCR and RNAi.

Primers	Sequences (5'-3')
RT-qPCR	
Rf β -Actin F	CCAAGGGAGCCAAGCAATT
Rf β -Actin R	CGCTGATGCCCTATGTATGT
RfCTL27 F	ATCAACGGATGGTTCTGGTC
RfCTL27 R	ACGAAGGGTTTCAGATGGT
RfAttacin F	TGGTTCTGGTGCCCAAGTGA
RfAttacin R	GCCATAACGATTCTTGTGGAGTA
RfCecropin F	CAGAAGCTGGTTGGTTGAAGA
RfCecropin R	GCAACACCGACATAACCCTGA
RfColeopericin F	TCGTGGTTTCTACCATGTTCACT
RfColeopericin R	TCAGCTAAAACCTGATCTTGGA
RfDefensin F	TTCGCCAAACTTATCCTCGTG
RfDefensin R	GGGTGCTTCGTTATCAACTTCC
RNAi	
RfdsCTL27 F	taatacgactcactatagggACCTGGAAGTCGACTGGTTG
RfdsCTL27 R	taatacgactcactatagggAGTTCCTCGTATCTTCGCA
RfdseGFP F	taatacgactcactatagggCAGTGCTTCAGCCGCTAC
RfdseGFP R	taatacgactcactatagggGTTACCTGCCGTTCTTGA

To assess whether the silencing of *RfCTL27* impacts both systemic and gut-localized immunity in RPW, we used enhanced green fluorescent protein (eGFP)-labeled *E. coli* as the pathogen and attacked RPW larvae by abdomen injection and oral feeding. The eGFP-labeled *E. coli* was prepared for the following treatments according to the method described in Section 2.4. The 4th instar larvae of RPWs injected with dsRNA were fed for 45 h. Then, 1 μL of suspensions containing eGFP-labeled *E. coli* was injected into the body cavity of RPW larvae. A total of 3 h later, 100 μL hemolymph was extracted in a laminar flow cabinet. The hemolymph was placed in a sterile EP tube containing 3 μL alpha-phenylthiourea (PTU) solution (5 mmol/L) and diluted 1000 times in sterile PBS gradient. A total of 150 μL of hemolymph was distributed on LB solid agar plates that were fortified with ampicillin. The plates were placed upside down in a 37 °C incubator for 12 h, and then the colony-forming units (CFUs) of eGFP-labeled *E. coli* were observed under a microscope. The CFUs were carefully counted to ensure accuracy. For feeding treatments, we selected healthy 4th instar larvae for our study. These larvae were starved for 12 h after injecting ds*RfCTL27* and then fed with fresh sugarcane slices containing 1 mL of eGFP-labeled *E. coli* suspension. A total of 24 h later, the guts were taken out and ground into homogenate in 1 mL sterile PBS. The homogenate was diluted 1000 times, 100 μL of the gut homogenate was poured on LB mediums containing ampicillin. The counting method was the same as above. Three biological replicates were set in each treatment, and each replicate contained four RPW larvae. In addition, 45 h after *RfCTL27* silencing, the expression levels of the four antimicrobial peptide genes *RfColeopteracin*, *RfCecropin*, *RfDefensin*, and *RfAttacin* were analyzed after injection of *E. coli*.

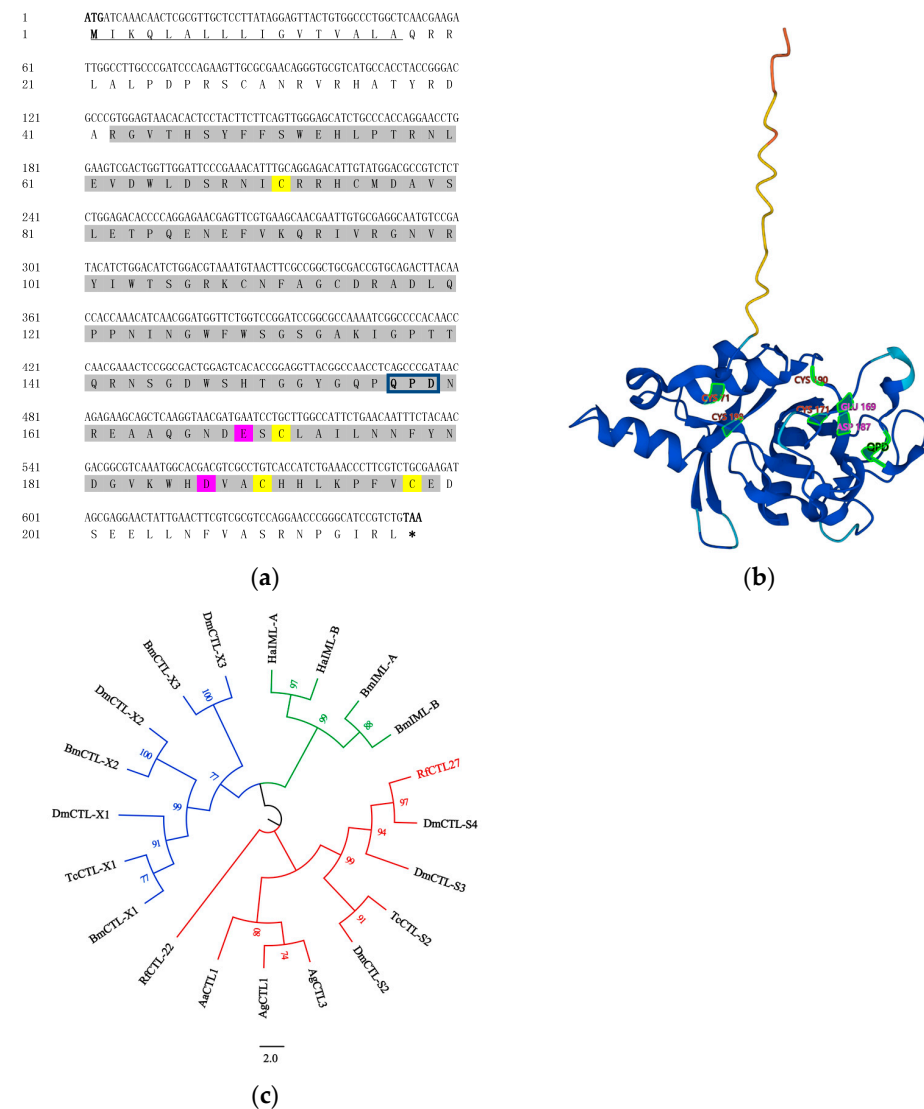
2.6. Data Analysis and Processing

The RNAi efficiency and other experiments were detected by *t*-test. One-way analysis of variance (ANOVA) was used to detect the expression of *RfCTL27* in different tissues and the effect of bacterial injection on the expression level of *RfCTL27*. GraphPad Prism 8.0.1 software was employed to data analysis and drawing. The data in the figures are expressed in the form of mean \pm SD.

3. Results

3.1. Sequence Characteristics of RfCTL27

The *RfCTL27* encoded a polypeptide, which is 217 residues long. The full length of *RfCTL27* was 1007 bp and ORF was 654 bp. *RfCTL27* contained two conserved functional domains, a carbohydrate recognition domain (CRD, 41–199 amino acids) and a signal peptide (1–17 amino acids), indicating that it belongs to the CTL-S family (Figure 1a). The binding specificity of *RfCTL27* mainly depends on the structural characteristics of CRDs. More interestingly, the Gln-Pro-Asp (QPD) motif was detected in *RfCTL27*, suggesting that it may recognize the pathogenic microorganisms, such as *E. coli*, by specifically binding mannose and galactose in their cell wall. Ca^{2+} binding sites were obtained by sequence alignment between *RfCTL27* and Rat MBP. The conserved Cysteine residues and two Ca^{2+} binding sites were discovered in CRD of *RfCTL27* (Figure 1a,b) and calcium ions were required for the binding activity of *RfCTL27*. Phylogenetic analysis showed that *RfCTL27* clustered with *DmCTL-S4*, *DmCTL-S3*, *DmCTL-S2*, and *TcCTL-S2* (Figure 1c). This suggests that *RfCTL27* is an orthologous protein in these species, indicating a shared evolutionary origin. Therefore, *RfCTL27* may have the same immune recognition function as CTL of *Drosophila melanogaster* Meigen and *Tribolium castaneum* (Herbst).



CRD; blue boxes indicate the position of the conserved domain species QPD motif; yellow shading represents Cysteine residue sites; and red shading represents Ca^{2+} ions binding sites. (b) Protein tertiary structure of RfCTL27. Red represents Cysteine residue sites; purple represents Ca^{2+} ions binding sites; and black font stands for QPD motif. (c) Phylogenetic analysis of RfCTL27 with other insect CTLs. Branches are color-coded: red, blue, and green represent members of the CTL-S, CTL-X, and IML series, respectively. The Genbank accession number are as follows: *Aedes aegypti* AaCTL1 (XP_021694337.1); *Anopheles gambiae* AgCTL1 (AGAP004811-PA); *Anopheles gambiae* AgCTL3 (EAA13236.4); *Bombyx mori* BmCTL-X1 (XP004932809.1); *Bombyx mori* BmCTL-X2 (XP004932837.1); *Bombyx mori* BmCTL-X3 (XP021204064.1); *Bombyx mori* BmIML-A (NP001165368.1); *Bombyx mori* BmIML-B (NP001165396.1); *Drosophila melanogaster* DmCTL-S2 (NP_001260046.1); *Drosophila melanogaster* DmCTL-S3 (NP_650179.1); *Drosophila melanogaster* DmCTL-S4 (NP_001260199.1); *Drosophila melanogaster* DmCTL-X1 (NP001096984.1); *Drosophila melanogaster* DmCTL-X2 (NP001285146.1); *Drosophila melanogaster* DmCTL-X3 (NP001245864.1); *Helicoverpa armigera* HaIML-A (XP021189909.1); *Helicoverpa armigera* HaIML-B (XP021190921.1); *Rhynchophorus ferrugineus* RfCTL22 (KAF7282966.1); *Rhynchophorus ferrugineus* RfCTL27 (KAF7272888.1); *Tribolium castaneum* TcCTL-S2 (XP_624536.2); and *Tribolium castaneum* TcCTL-X1 (XP015833550.1).

3.2. Expression Profiles of RfCTL27 in the Tissues of RPW Larvae

RT-qPCR assays showed that RfCTL27 presented with significantly different expression levels in multiple tissues of RPW larvae, such as the head, cuticle, foregut, mid- and hindgut, fat body, and hemolymph (ANOVA: $F_{5,18} = 4.24$, $p < 0.05$). Notably, the expression level of RfCTL27 was significantly higher in the gut and fat body than in the head, cuticle, and hemolymph (Figure 2), implying that RfCTL27 might play some important roles in the local and systemic immunity of RPW larvae.

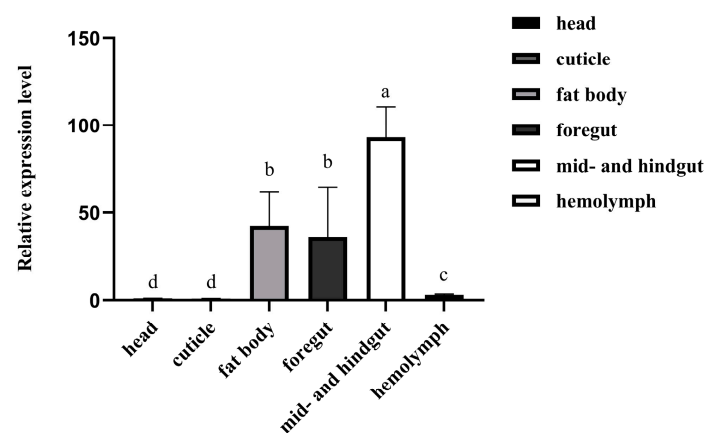


Figure 2. The expression profiles of RfCTL27 in different tissues of RPW larvae. Four RPW larvae composed of a biological replicate, and three biological replicates were included in each treatment. Rfβ-Actin served as the internal reference gene. The data in the figure are represented by mean ± SD. Lowercase letters above bars indicate significance across different tissues (one-way analysis of variance (ANOVA) test, $p < 0.05$).

3.3. Expression Patterns of RfCTL27 upon Pathogen Challenge in RPW Larvae

After 6 h of *E. coli* injection, the expression level of RfCTL27 in the gut of RPW larvae was significantly higher than that in other groups, i.e., 12 h and 24 h after *E. coli* challenge (ANOVA: $F_{2,6} = 9.71$, $p = 0.013$, Figure 3a). In fat body, the expression level of RfCTL27 was significantly elevated at 12 h after the infection of *E. coli* in contrast with the phosphate-buffered saline (PBS) and *S. aureus* group (ANOVA: $F_{2,6} = 43.36$, $p = 0.029$, Figure 3b). Furthermore, the expression level of RfCTL27 in fat body at 12 h after the challenge of *E. coli* was significantly higher than that of two other timepoints (ANOVA: $F_{2,6} = 30.67$, $p = 0.043$, Figure 3b). However, the injection of *S. aureus* into the hemocoel of RPW larvae did not increase the expression level of RfCTL27 in fat body (ANOVA: $F_{2,6} = 1.46$, $p = 0.31$,

Figure 3b). Totally, these results suggest that *E. coli* infection can affect the expression level of *RfCTL27* in the gut of RPWs, and *RfCTL27* in the fat body of RPWs may be involved in mediating the systemic immune response of the insect against Gram-negative bacteria.

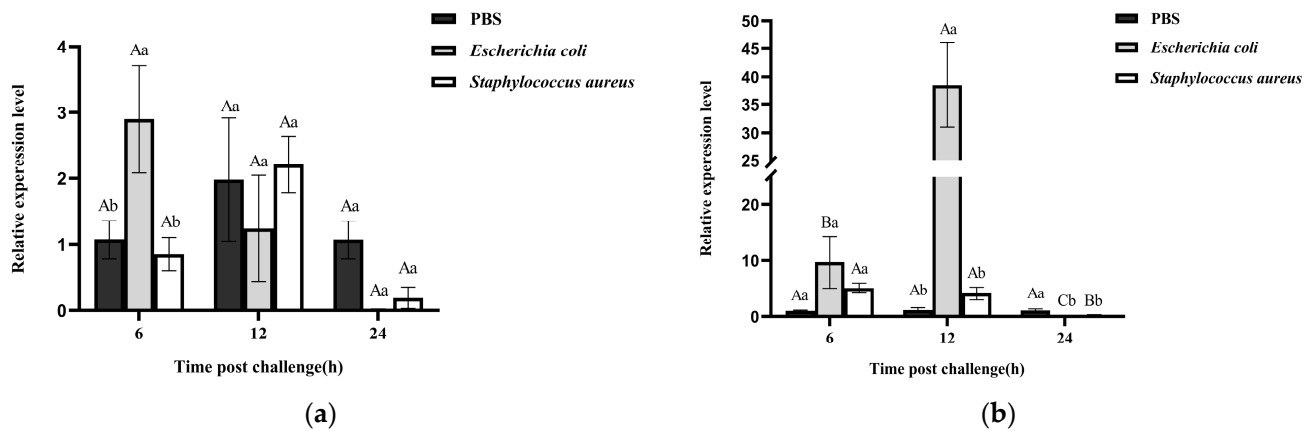


Figure 3. Changes in the expression level of *RfCTL27* in the (a) gut and (b) fat body of the RPW larvae upon challenge with *E. coli* and *S. aureus* by injection. Each larva was injected with 1 μ L bacterial suspension, four RPW larvae composed of a biological replicate, and three biological replicates were included in each treatment. *Rf β -Actin* served as the internal reference gene. Phosphate-buffered saline (PBS) was injected as a control. The data in the figure are represented by mean \pm SD. Different capital and lowercase letters above bars represent significance in the gene expression level between different time points in the same treatments and across the different treatments at the same time point, respectively (one-way analysis of variance (ANOVA) test, $p < 0.05$).

3.4. Effect of *RfCTL27* Silencing on the Immunocompetence of RPW Larvae and Expression of Antimicrobial Peptide Genes in the Gut and Fat Body

After 48 h of dsRNA delivery into the body cavity of RPW larvae, the expression levels of *RfCTL27* in the gut and fat body were significantly reduced. The expression level in the gut was significantly dropped by 96.20% (t -test: $t = 7.12$, $p < 0.01$), while that in the fat body was significantly dropped by 74.40% (t -test: $t = 6.05$, $p < 0.01$) (Figure 4). Moreover, a significant decrease in the relative expression level of the antimicrobial peptide *Rfcecropin* was detected in the gut of RPW larvae (t -test: $t = 3.31$, $p < 0.05$, Figure 5a). More interestingly, the number of eGFP-labeled *E. coli* colonies (CFU) was $12,500.00 \pm 1946.79$ in the gut of the fourth instar larvae of the RPW after RNAi interference with *RfCTL27*, while that of the control group was 7233.33 ± 550.76 (Figure 6). The number of the *dsRfCTL27* group was significantly higher than that of the *dseGFP* group (t -test: $t = 4.51$, $p < 0.05$), indicating that *RfCTL27* silencing significantly impaired the ability of the gut to eliminate the invaded pathogenic bacteria by oral feeding. These results suggested that RPW gut immunocompetence was compromised by the knockdown of *RfCTL27* to reduce the expression level of *RfCecropin*.

3.5. The Effect of *RfCTL27* Knockdown on the Ability of RPW Larvae to Clear to the Invaded *E. coli* in Hemolymph

In the group of *RfCTL27* silencing, $16,146.67 \pm 515.88$ eGFP-labeled *E. coli* colonies (CFU) were recovered from the hemolymph of RPW larvae, but that of the control group was 7953.33 ± 853.31 (Figure 7). Statistical analysis revealed that the number of eGFP-labeled *E. coli* colonies in *RfCTL27*-silenced insects was significantly greater than that of controls (t -test: $t = 14.23$, $p < 0.05$). In fat body, the relative expression level of *RfDefensin* was also significantly decreased compared with the control group (t -test: $t = 3.51$, $p < 0.05$, Figure 5b), suggesting that the systemic immunity of this pest was impaired by *RfCTL27* silencing.

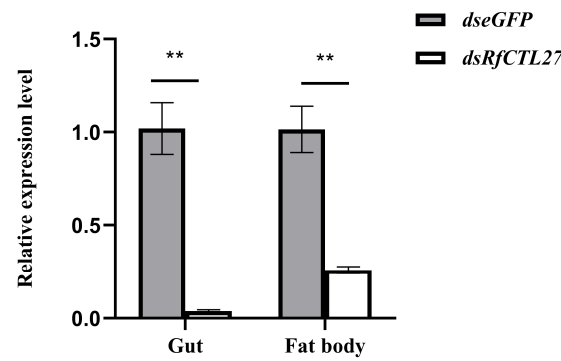


Figure 4. RNAi efficiency of *RfCTL27* in the gut and fat body of RPW larvae. *dsRfCTL27* represents the group for silencing *RfCTL27*. *dseGFP* served as the control by the delivery of double-strand *eGFP* RNA. Four RPW larvae composed of a biological replicate, and three biological replicates were included in each treatment. *Rfβ-Actin* served as the internal reference gene. The data in the figure are represented by mean ± SD. Asterisk above bars indicates significant difference in the figure between the two groups (*t*-test, $p < 0.001$).

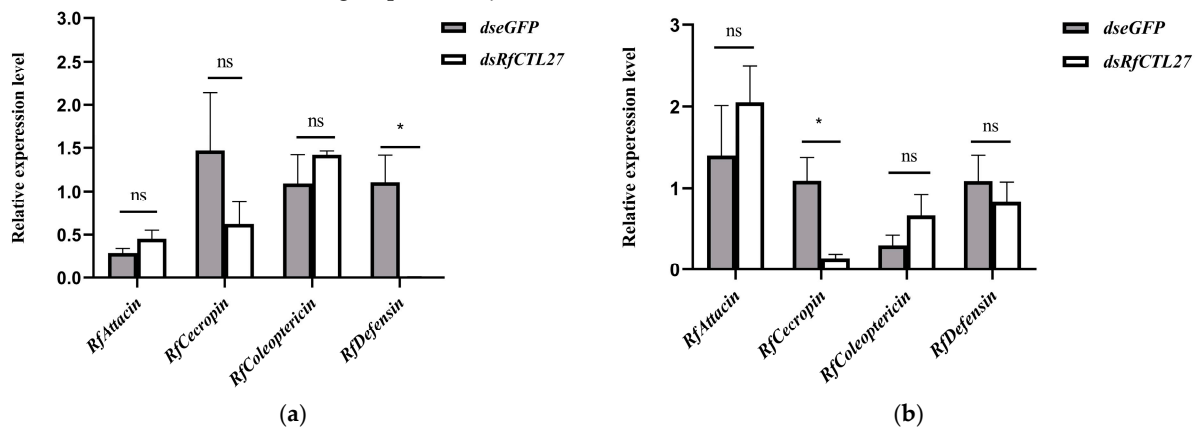


Figure 5. Effect of RNAi of *RfCTL27* on the expression levels of four AMP genes in the (a) gut and (b) fat body of RPW larvae. *dsRfCTL27* represents the group for silencing *RfCTL27*. *dseGFP* served as the control by the delivery of double-strand *eGFP* RNA. Four RPW larvae composed of a biological replicate, and three biological replicates were included in each treatment. *Rfβ-Actin* served as the internal reference gene. The data are represented by mean ± SD. ns represents no significance in the expression level of AMP genes between the two treatments. Asterisk above bars indicates significance between the two groups (*t*-test, $p < 0.05$).

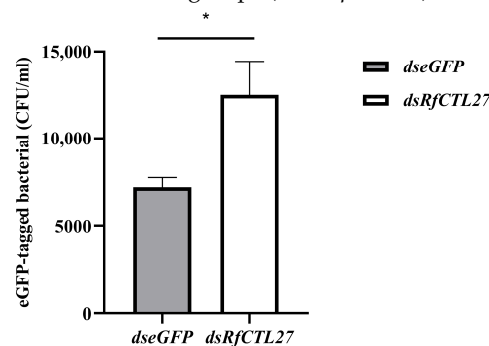


Figure 6. The effect of *RfCTL27* knockdown on the persistence of introduced eGFP-labeled *E. coli* in the gut of RPW larvae. *dsRfCTL27* represents the group for silencing *RfCTL27*. *dseGFP* served as the control by the delivery of double-strand *eGFP* RNA. Four RPW larvae composed of a biological replicate, and three biological replicates were included in each treatment. *Rfβ-Actin* served as the internal reference gene. The data in the figure are represented by mean ± SD. Asterisk above bars indicates significance in the figure between the two groups (*t*-test, $p < 0.05$).

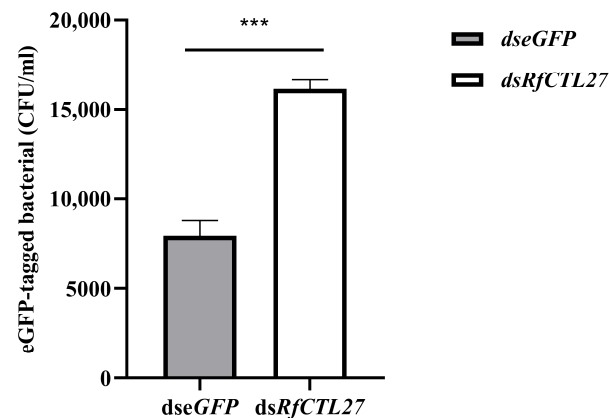


Figure 7. Effect of *RfCTL27* knockdown on the removing of injected eGFP-labeled *E. coli* of hemolymph in RPW larvae. *dsRfCTL27* represents the group for silencing *RfCTL27*. *dseGFP* served as the control by the delivery of double-strand eGFP RNA. Four RPW larvae composed of a biological replicate, and three biological replicates were included in each treatment. *Rfβ-Actin* served as the internal reference gene. The data in the figure are represented by mean \pm SD. Asterisk above bars indicates significance between the two groups (*t*-test, $p < 0.0001$).

4. Discussion

Many studies have indicated an increase in *R. ferrugineus* immune resistance under the influence of infection with various microorganisms [1,8]. However, the mechanisms underlying how the immune system of RPWs detects and discriminates the invaded microbes have been mostly elusive. In invertebrates, CTLs have been shown to recognize bacteria and mediate immune responses [16,17]. Here, we found that *RfCTL27* encodes a polypeptide of 217 amino acids with two conserved functional domains, a CRD (41–199 amino acids) and a signal peptide (1–17 amino acids). The three-dimensional structure of *RfCTL27* is a canonical fold, consisting of α -helices, β -sheets, and loops. This fold is stabilized by two pairs of disulfide bonds between Cys (71) and Cys (198), as well as Cys (171) and Cys (190). RT-qPCR analysis showed that the expression levels of *RfCTL27* in the gut and fat body of RPW larvae were significantly higher than that in other tissues. For insects, fat body and gut are the important immune organs, which are involved in the systemic and local immunity, respectively [18,19]. Consequently, the higher expression level of *RfCTL27* in these two tissues strongly suggest that *RfCTL27* might have vital immune functions. More specifically, our data indicated that the challenge of Gram-negative bacterium *E. coli* dramatically enhanced the expression of *RfCTL27* in the fat body and gut of RPW larvae compared with other treatments. The conservative functional domain, a QPD motif, was found in *RfCTL27*, which can specifically bind to galactose-type carbohydrates, peptidoglycan and lipopolysaccharide on the surface of bacterial wall [10,20–24]. Collectively, these results show that *RfCTL27* acts as a PRR to participate in the immune responses of this pest by the discrimination of Gram-negative bacterium.

After *RfCTL27* was silenced, we find that the ability of RPW larvae gut and hemolymph to clear eGFP-labeled *E. coli* was significantly reduced through biological experiments. Furthermore, we found that the silencing of *RfCTL27* led to a significant dropping in the expression level of two antimicrobial peptide genes, *RfCecropin* in the gut and *RfDefensin* in the fat body of RPW larvae. The antimicrobial peptides are the pivotal effectors for animals to clear the non-self objects including pathogenic bacteria and virus. Two antimicrobial peptides, Defensin and Cecropin, were identified in *Anopheles gambiae*, and Defensin was found to have antibacterial activity against *E. coli* [25–27]. In *Drosophila melanogaster*, the antimicrobial peptide Cecropin had stronger bactericidal activity against Gram-negative bacterium *E. coli* compared to Gram-positive bacterium *S. aureus* [28]. Consequently, these data evidently indicated that *RfCTL27* was concerned with the activation of AMP genes in this pest. The homeostasis of intestinal microbiota largely determines the healthy status of

animal hosts [10,19]. CTLs modulate gut microbiome homeostasis by coating the bacterial surface to counteract AMP activity bacteria [29]. More specifically, the CTL24 protein prevents the continuous elimination of gut commensal bacteria, maintaining homeostasis by reducing LysC-mediated muropeptide release and AlfB1's bacterial activity in shrimp [30]. In the current study, our results implied that *RfCTL27* could regulate gut immunity by the modulation of AMP expression. However, the mechanisms of how *RfCTL27* mediates the production of antimicrobial peptides and intestinal homeostasis are still unclear. In conclusion, our findings indicate that *RfCTL27* is related to the systemic and gut local immunity by regulating the expression of AMP genes under the exposure of Gram-negative bacteria.

Author Contributions: Z.S. (Zhanghong Shi) and Y.H. provided resources; Z.S. (Zhanghong Shi) conceived and designed the research; Y.G., Y.X., Z.S. (Zhiping Su), X.W., Y.K. and B.M. completed the experiments; Y.X., X.W., Z.S. (Zhiping Su) and B.M. analyzed the data; Y.G., Y.X. and Z.S. (Zhanghong Shi) wrote the article. All authors have read and agreed to the published version of the manuscript.

Funding: This research was funded by the National Natural Science Foundation of China (31470656), Natural Science Foundation of Fujian Province (2021J01068, 2018J01705), the Special Natural Science Foundation of Fujian Agriculture and Forestry University (CXZX2019002G), and the Program for New Century Excellent Talents in University of Fujian Province (KLa16058A).

Data Availability Statement: The data presented in this study are available on request from the corresponding author.

Conflicts of Interest: The authors declare no conflicts of interest.

References

1. Knutelski, S.; Awad, M.; Łukasz, N.; Bukowski, M.; Śmiałek, J.; Suder, P.; Dubin, G.; Mak, P. Isolation, identification, and bioinformatic analysis of antibacterial proteins and peptides from immunized hemolymph of red palm weevil *Rhynchophorus ferrugineus*. *Biomolecules* **2021**, *11*, 83. [\[CrossRef\]](#)
2. Shar, M.U.; Rustamani, M.A.; Nizamani, S.M.; Bhutto, L.A. Red palm weevil (*Rhynchophorus ferrugineus* Olivier) infestation and its chemical control in Sindh province of Pakistan. *Afr. J. Agric. Res.* **2012**, *7*, 1666–1673.
3. Habib, D.M.; Mouna, N.C.I.B.; Wiem, H. Red palm weevil (*Rhynchophorus ferrugineus*) chemical treatments applied on ornamental palms in Tunisia: Results of extensive experiments. *Int. J. Agric. Innov. Res.* **2017**, *5*, 1062–1068.
4. Pu, Y.C.; Ma, T.L.; Hou, Y.M.; Sun, M. An entomopathogenic bacterium strain, *Bacillus thuringiensis*, as a biological control agent against the red palm weevil, *Rhynchophorus ferrugineus* (Coleoptera: Curculionidae). *Pest Manag. Sci.* **2017**, *73*, 1494–1502. [\[CrossRef\]](#) [\[PubMed\]](#)
5. Muhammad, A.; Habineza, P.; Ji, T.; Hou, Y.; Shi, Z. Intestinal microbiota confer protection by priming the immune system of red palm weevil *Rhynchophorus ferrugineus* Olivier (Coleoptera: Dryophthoridae). *Front. Physiol.* **2019**, *10*, 1303. [\[CrossRef\]](#) [\[PubMed\]](#)
6. Dembilio, Ó.; Quesada-Moraga, E.; Santiago-Álvarez, C.; Jacas, J.A. Potential of an indigenous strain of the entomopathogenic fungus *Beauveria bassiana* as a biological control agent against the Red Palm Weevil, *Rhynchophorus ferrugineus*. *J. Invertebr. Pathol.* **2010**, *104*, 214–221. [\[CrossRef\]](#) [\[PubMed\]](#)
7. Hazzouri, K.M.; Sudalaimuthasari, N.; Kundu, B.; Nelson, D.; Al-Deeb, M.A.; Le Mansour, A.; Amiri, K.M. The genome of pest *Rhynchophorus ferrugineus* reveals gene families important at the plant-beetle interface. *Commun. Biol.* **2020**, *3*, 323. [\[CrossRef\]](#) [\[PubMed\]](#)
8. Hussain, A.; Rizwan-ul-Haq, M.; Al-Ayedh, H.; AlJabr, A.M. Susceptibility and immune defence mechanisms of *Rhynchophorus ferrugineus* (Olivier) (Coleoptera: Curculionidae) against entomopathogenic fungal infections. *Int. J. Mol. Sci.* **2016**, *17*, 1518. [\[CrossRef\]](#)
9. Ma, B.; Wang, X.; Liu, Q.; Zhao, Y.; Su, Z.; Chen, Y.; Shi, Z. A peptidoglycan recognition protein regulates the immune response of *Rhynchophorus ferrugineus* Olivier (Coleoptera: Dryophthoridae) during exposure to pathogenic Gram-positive bacteria and fungi. *Dev. Comp. Immunol.* **2023**, *144*, 104705. [\[CrossRef\]](#)
10. Brown, G.D.; Willment, J.A.; Whitehead, L. C-type lectins in immunity and homeostasis. *Nat. Rev. Immunol.* **2018**, *18*, 374–389. [\[CrossRef\]](#)
11. Li, J.; Bi, J.; Zhang, P.; Wang, Z.; Zhong, Y.; Xu, S.; Wang, L.; Li, B. Functions of a C-type lectin with a single carbohydrate-recognition domain in the innate immunity and movement of the red flour beetle, *Tribolium castaneum*. *Insect. Mol. Biol.* **2019**, *30*, 90–101. [\[CrossRef\]](#) [\[PubMed\]](#)
12. Tanji, T.; Ohashi-Kobayashi, A.; Natori, S. Participation of a galactose-specific C-type lectin in *Drosophila* immunity. *Biochem. J.* **2006**, *396*, 127–138. [\[CrossRef\]](#) [\[PubMed\]](#)
13. Yu, X.Q.; Kanost, M.R. Immulectin-2, a lipopolysaccharide-specific lectin from an insect, *Manduca sexta*, is induced in response to gram-negative bacteria. *J. Biol. Chem.* **2000**, *275*, 37373–37381. [\[CrossRef\]](#) [\[PubMed\]](#)

14. Zhan, M.Y.; Shahzad, T.; Yang, P.J.; Liu, S.; Yu, X.Q.; Rao, X.J. A single-CRD C-type lectin is important for bacterial clearance in the silkworm. *Dev. Comp. Immunol.* **2016**, *65*, 330–339. [[CrossRef](#)] [[PubMed](#)]
15. Lu, Y.; Su, F.; Zhu, K.; Zhu, M.; Li, Q.; Hu, Q.; Yu, X.Q. Comparative genomic analysis of C-type lectin-domain genes in seven holometabolous insect species. *Insect. Biochem. Mol. Biol.* **2020**, *126*, 103451. [[CrossRef](#)]
16. Li, M.; Li, C.; Ma, C.; Li, H.; Zuo, H.; Weng, S.; Chen, X.; Zeng, D.; He, J.; Xu, X. Identification of a C-type lectin with antiviral and antibacterial activity from pacific white shrimp *Litopenaeus vannamei*. *Dev. Comp. Immunol.* **2014**, *46*, 231–240. [[CrossRef](#)]
17. Ling, E.; Ao, J.; Yu, X.Q. Nuclear translocation of immulectin-3 stimulates hemocyte proliferation. *Mol. Immunol.* **2008**, *45*, 2598–2606. [[CrossRef](#)]
18. Lemaitre, B.; Hoffmann, J. The host defense of *Drosophila melanogaster*. *Annu. Rev. Immunol.* **2007**, *25*, 697–743. [[CrossRef](#)]
19. Muhammad, A.; Habineza, P.; Wang, X.; Xiao, R.; Ji, T.; Hou, Y.; Shi, Z. Spätzle Homolog-Mediated Toll-Like Pathway Regulates Innate Immune Responses to Maintain the Homeostasis of Gut Microbiota in the Red Palm Weevil, *Rhynchophorus ferrugineus* Olivier (Coleoptera: Dryophthoridae). *Front. Microbiol.* **2020**, *11*, 846. [[CrossRef](#)] [[PubMed](#)]
20. Zelensky, A.N.; Gready, J.E. The C-type lectin-like domain superfamily. *FEBS J.* **2005**, *272*, 6179–6217. [[CrossRef](#)] [[PubMed](#)]
21. Weis, W.I.; Kahn, R.; Fourme, R.; Drickamer, K.; Hendrickson, W.A. Structure of the calcium-dependent lectin domain from a rat mannose-binding protein determined by MAD phasing. *Science* **1991**, *254*, 1608–1615. [[CrossRef](#)]
22. Yu, X.Q.; Ma, Y. Calcium is not required for immulectin-2 binding, but protects the protein from proteinase digestion. *Insect. Biochem. Mol. Biol.* **2006**, *36*, 505–516. [[CrossRef](#)] [[PubMed](#)]
23. Zhang, H.; Wang, H.; Wang, L.; Song, X.; Zhao, J.; Qiu, L.; Li, L.; Song, L. A novel C-type lectin (Cflec-3) from *Chlamys farreri* with three carbohydrate-recognition domains. *Fish. Shellfish. Immunol.* **2009**, *26*, 707–715. [[CrossRef](#)]
24. Huang, X.; Huang, Y.; Shi, Y.R.; Ren, Q.; Wang, W. Function of a novel C-type lectin with two CRD domains from *Macrobrachium rosenbergii* in innate immunity. *Dev. Comp. Immunol.* **2015**, *49*, 121–126. [[CrossRef](#)] [[PubMed](#)]
25. Jacopo, V.; Adam, M.; Richma, B.; Sandrine, U.; Claudia, B.; Philippe, B. The defensin peptide of the malaria vector mosquito *Anopheles gambiae*: Antimicrobial activities and expression in adult mosquitoes. *Insect. Biochem. Mol.* **2001**, *31*, 241–248.
26. Vizioli, J.; Bulet, P.; Charlet, M.; Lowenberger, C.; Blass, C.; Müller, H.M.; Dimopoulos, G.; Hoffmann, J.; Kafatos, F.C.; Richman, A. Cloning and analysis of a cecropin gene from the malaria vector mosquito, *Anopheles gambiae*. *Insect. Mol. Biol.* **2000**, *9*, 75–84. [[CrossRef](#)] [[PubMed](#)]
27. Richman, A.M.; Bulet, P.; Hetru, C.; Barillas, M.C.; Hoffmann, J.A.; Kafatos, F.C. Inducible immune factors of the vector mosquito *Anopheles gambiae*: Biochemical purification of a defensin antibacterial peptide and molecular cloning of preprodefensin cDNA. *Insect. Mol. Biol.* **1996**, *5*, 203–210. [[CrossRef](#)] [[PubMed](#)]
28. Samakovlis, C.; Kimbrell, D.A.; Kylsten, P.; Engström, A.; Hultmark, D. The immune response in *Drosophila*: Pattern of cecropin expression and biological activity. *EMBO J.* **1990**, *9*, 2969–2976. [[CrossRef](#)]
29. Pang, X.; Xiao, X.; Liu, Y.; Zhang, R.; Liu, J.; Liu, Q.; Wang, P.; Cheng, G. Mosquito C-type lectins maintain gut microbiome homeostasis. *Nat. Microbiol.* **2016**, *1*, 16023. [[CrossRef](#)]
30. Liu, P.P.; Wei, Z.; Cheng, Z.H.; Wang, X.W. Small immune effectors coordinate peptidoglycan-derived immunity to regulate intestinal bacteria in shrimp. *PLoS Pathog.* **2022**, *18*, e1010967. [[CrossRef](#)]

Disclaimer/Publisher’s Note: The statements, opinions and data contained in all publications are solely those of the individual author(s) and contributor(s) and not of MDPI and/or the editor(s). MDPI and/or the editor(s) disclaim responsibility for any injury to people or property resulting from any ideas, methods, instructions or products referred to in the content.